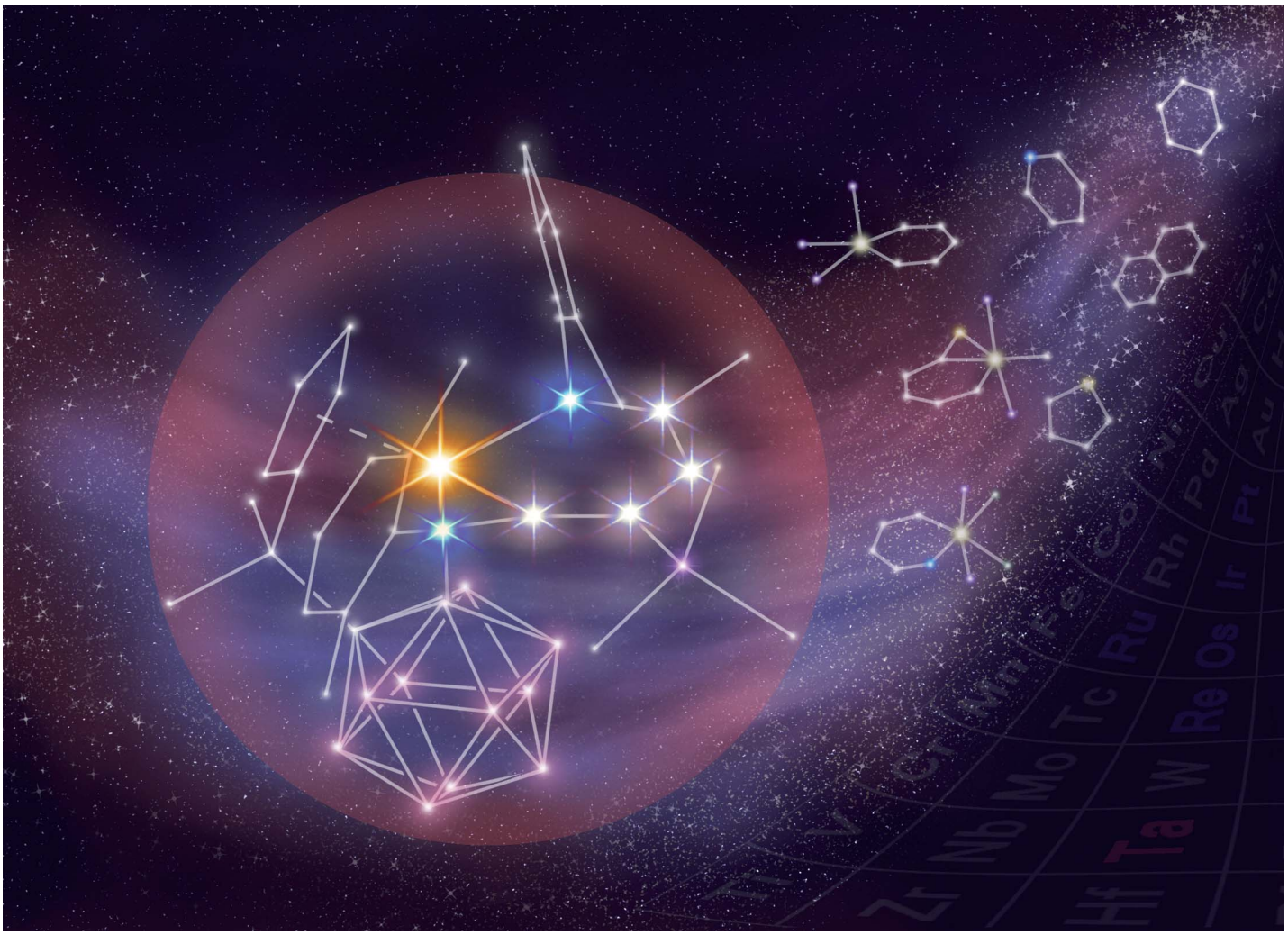

Showcasing research from Professor Xie's laboratory, Department of Chemistry, The Chinese University of Hong Kong, Shatin NT, Hong Kong, China.

Metallaaromaticity involving a d^0 early transition metal centre: synthesis, structure, and aromaticity of tantallapyridinazirine complexes

Though late transition metal aromatic metallabenzenes and related heteroatom-containing analogues have been well studied, the corresponding aromatic early transition metal complexes remain elusive. This paper describes the synthesis of aromatic, planar, and delocalised organotantallapyridinium complexes, which represents a class of long-sought-after molecules.

As featured in:

See Zhenyang Lin, Zuowei Xie *et al.*, *Chem. Sci.*, 2024, **15**, 7943.

ROYAL SOCIETY OF CHEMISTRY

rsc.li/chemical-science

Registered charity number: 207890

Chemical Science

ROYAL SOCIETY OF CHEMISTRY

EDGE ARTICLE

View Article Online
View Journal | View Issue

Check for updates

Cite this: *Chem. Sci.*, 2024, **15**, 7943

All publication charges for this article have been paid for by the Royal Society of Chemistry

Received 20th April 2024
Accepted 3rd May 2024

DOI: 10.1039/d4sc02629b

rsc.li/chemical-science

Metallaaromaticity involving a d^0 early transition metal centre: synthesis, structure, and aromaticity of tantallapyridinazirine complexes†

Jingting Yang,‡[a] Xin Xu,‡[b] Zhenyang Lin *[b] and Zuowei Xie *[ac]

Though late transition metal aromatic metallabenzenes and related heteroatom-containing analogues have been well studied, the corresponding aromatic early transition metal complexes remain elusive. Herein, we demonstrate the synthesis of aromatic, planar, and delocalised organotantallapyridinium complexes *via* a simple one-pot process by sequential treatment of tantalum methyl complex [η^5:σ-$Me_2C(C_5H_4)(C_2B_{10}H_{10})$]$TaMe_3$ with alkynes and isocyanide. Single-crystal X-ray analyses, NMR spectroscopic data and DFT calculations suggest that they are aromatic tantallapyridinium complexes, a class of long-sought-after molecules. This work would shed some light on the preparation of metallaaromatics involving early transition metals.

Introduction

Aromatic chemistry has fascinated chemists for almost two centuries since Faraday isolated benzene in 1825,[1] and Kekulé proposed his famous structure of benzene in 1865.[2] Replacement of one CH unit in the aromatic system with an isolobal organometallic fragment delivers a class of metallaaromatic compounds, which have aroused significant synthetic and theoretical interest, for they are expected to possess both aromatic and organometallic properties,[3] and extending the boundary and criteria of aromaticity.[4] Represented by metallabenzene and metallabenzynes, a vast array of metallaaromatic compounds have been synthesised and characterised, varying in sizes of metallacycles, topologies of polycyclic structures (fused and spiro), types of aromaticity-contributing orbitals (π, σ), and the presence of heteroatoms or not.[5] However, very narrow scope of metals is known to form isolable metallaaromatic compounds so far,[5] dominated by late transition metals (Chart 1).[6,7] In 2021, Xi and co-workers reported two examples of aromatic, anionic tris-spiro metalloles of V and Cr with d^5 electron configuration, representing scarce examples of early transition metallaaromatic compounds.[8] Still, aromatic metallacycles involving d^0 metal ions remain unknown.

Challenges in synthesising early transition metal-containing metallaaromatic systems, specifically aromatic metallabenzenes and heterometallabenzenes, are encountered from both experimental and theoretical aspects. Experimentally, the oxophilicity of d^0 early transition metal complexes complicates their purification, excluding column chromatography. DFT (density functional theory) studies suggested that d^0-metallabenzenes and related compounds, d^0-metallapyrimidines, exhibit antiaromatic properties.[9] The few isolable examples of d^0-heterometallabenzenes show no convincing aromatic patterns, as evidenced by bond-length alternation and short M–N lengths (Chart 2).[10] The only case of d^0-metallabenzene,

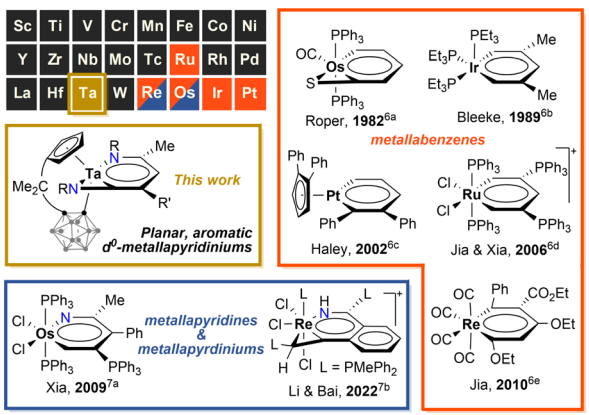

Chart 1 Selected examples of aromatic metallabenzenes, metallapyridines and metallapyridiniums. The coloured boxes represent the elements that are known to form aromatic metallabenzenes (in orange) or metallapyridines/pyridiniums (in navy).

[a]*Department of Chemistry, State Key Laboratory of Synthetic Chemistry, The Chinese University of Hong Kong, Shatin, New Territories, Hong Kong, China*

[b]*Department of Chemistry, The Hong Kong University of Science and Technology, Clear Water Bay, Kowloon, Hong Kong, China*

[c]*Shenzhen Grubbs Institute, Department of Chemistry, Southern University of Science and Technology, Shenzhen 518055, China*

† Electronic supplementary information (ESI) available: Experimental procedures, complete characterisation data, computational details, and NMR spectra. CCDC 2288668–2288670 for **5–7**, respectively. For ESI and crystallographic data in CIF or other electronic format see DOI: https://doi.org/10.1039/d4sc02629b

‡ These authors contributed equally to this article.

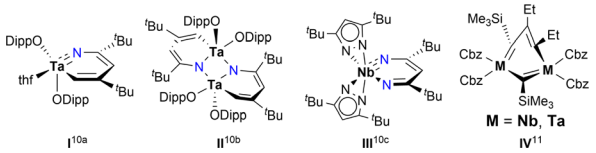

Chart 2 Selected examples of nonaromatic d^0-metallabenzenoids.

1,3-dimetallabenzenes (M = Nb, Ta), presents a twisted nonplanar structure (Chart 2).[11] These observations seem to point to the inaccessibility of aromatic d^0-metallabenzenoids. Thus, aromatic metallabenzene and its heteroatomic analogues containing d^0 early transition metals have become long-sought-after molecules.

During our study on organotantalum alkyne complexes bearing a multidentate bulky $[Me_2C(C_5H_4)(C_2B_{10}H_{10})]^{2-}$ ligand, we observed sequential insertion-C–C coupling reactions with unsaturated molecules on a Ta(v) metal centre, facilely yielding a variety of d^0-tantalum metallacycles.[12] Based on these results, we speculate that the steric bulkiness of the σ-carboranyl ligand can effectively protect the electrophilic metal centre during multi-step insertion reactions, facilitating the formation of large metallacycles.[13] To our delight, the multiple insertions of isocyanides into alkyl tantalum–alkyne complexes $[\eta^5{:}\sigma\text{-}Me_2C(C_5H_4)(C_2B_{10}H_{10})]TaMe(\eta^2\text{-}RC{\equiv}CH)$ delivered an unprecedented class of tantallapyridinazirine complexes, of which the tantallapyridinium ring manifests aromatic characters. The synthesis can be conveniently accomplished *via* a one-pot process from the easily prepared tantalum methyl complex $[\eta^5{:}\sigma\text{-}Me_2C(C_5H_4)(C_2B_{10}H_{10})]TaMe_3$.[14] To the best of our knowledge, it is the first example of aromatic d^0-heterometallabenzene involving an early transition metal. Our findings are detailed in this article.

Results and discussion

Synthesis and characterisation

The starting material, tantalum methyl complex $[\eta^5{:}\sigma\text{-}Me_2C(C_5H_4)(C_2B_{10}H_{10})]TaMe_3$ (**1**), was conveniently synthesised *via* a salt metathesis method.[14] The organotantalum alkynes complexes $[\eta^5{:}\sigma\text{-}Me_2C(C_5H_4)(C_2B_{10}H_{10})]TaMe(\eta^2\text{-}RC{\equiv}CH)$ [R = $SiMe_3$ (**2**), ^{t}Bu (**3**), ^{p}Tol (**4**)] were freshly prepared *via* the hydrogenolysis of **1** in the presence of the corresponding alkynes.[12] Treatment of *in situ* formed **2** with two equiv. of 2,6-dimethylphenyl isocyanide (XylNC) in toluene at room temperature afforded complex **5** in 75% isolated yield. Similarly, complexes **6** and **7** were prepared in 30% and 68% yields, respectively (Scheme 1). The lower yield of **6** could be ascribed to the steric hindrance of the *t*-butyl group.

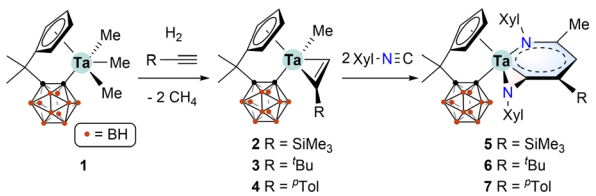

Scheme 1 Synthesis of tantalum alkyne complexes **2–4** and tantallapyridinazirine complexes **5–7**.

These complexes were stable under an inert atmosphere; however, they were moisture-sensitive. They were isolated as dark brown crystals and well-characterised by single-crystal X-ray analyses and NMR spectroscopy.

Single-crystal X-ray analyses show that **5–7** share a similar core structure in which the tantalum atom is η^5-bound to the cyclopentadienyl ring, σ-bound to the carboranyl cage carbon, and incorporated into a bicyclic framework consisting of a tantallapyridinium unit and a tantallaazirine moiety. The representative structure of **5** is shown in Fig. 1. The molecular structures of **6** and **7** are included in the ESI (Fig. S2 and S3†). As the key structural parameters in **5–7** are very close, we chose **5** as an example for detailed discussions.

Taking a close look at the bonding within the metallabicyclic moiety of **5**, the Ta(1)–C(3) bond length (2.031(4) Å) falls at the longer end of Ta–C lengths for typical Schrock-type Ta–alkylidene complexes (1.920(6)–2.030(6) Å)[15] and is shorter than a normal Ta–C(sp^2) single bond (2.147(8) Å) in a tantallacyclopentadiene complex,[16] suggesting some double bond character. The exocyclic Ta(1)–N(1) (1.992(3) Å) length is comparable with those found in Ta–amide complexes, and the trigonal planar geometry around N(1) is indicative of $Ta(d_\pi) \leftarrow N(p_\pi)$ interaction.[17] The Ta(1)–N(2) bond length of 2.107(3) Å is longer than the Ta(1)–N(1) one but is still within the range of Ta–N σ-bond lengths with considerable $d_\pi \leftarrow p_\pi$ donation;[18] the longer metal–nitrogen linkage is probably due to the steric repulsion between the bulky xylyl group and the carboranyl ligand. The C(3)–C(4)/C(4)–C(5)/C(5)–C(6) bond lengths (1.357(5)/1.424(6)/1.381(5) Å) are intermediate between those of typical C–C single and C=C double bonds, showing some extent of bond length equalisation, and the range of the C–C lengths in **5** shows a smaller spread than those of tantallapyridine **I** (1.35(2)–1.45(2) Å) and tantallapyridine dimer **II** (1.343(6)–1.454(7) Å) (Chart 2), which share a similar TaC_4N metallacycle moiety.[10a,b] Note that a slight extent of C–C bond length alternation is commonly observed in metallaaromatic systems, such as in a rhenabenzene (1.354(5)–1.444(5) Å).[6e]

The solution NMR data for characteristic metallacyclic signals in **5–7** in C_6D_6 are compiled in Table 1, and we chose **5** for discussion. In the ^{1}H NMR spectrum of **5**, the metallacyclic

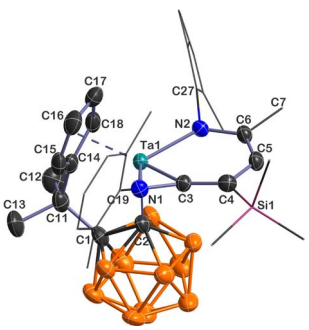

Fig. 1 Solid-state structure of **5** drawn at the 50% probability level. For clarity, the xylyl and $SiMe_3$ moieties are drawn in a wireframe, and the hydrogen atoms are omitted.

Table 1 Selected ^{1}H NMR and ^{13}C{^{1}H} NMR chemical shifts (δ in ppm) for **5–7**[a]

	^{1}H NMR		^{13}C{^{1}H} NMR			
	C^5–*H*	C^6–CH_3	C^3	C^4	C^5	C^6
5	6.83	2.19	222.4	92.7	127.9	141.7
6	6.83	2.17	210.1	113.2	123.7	143.7
7	7.05	2.17	213.5	105.9	122.7	145.3

[a] For the atomic labels, see Fig. 1.

$C_\gamma(5)$–*H* proton was observed at 6.83 ppm as a singlet. The corresponding 6.83 and 7.05 ppm chemical shifts were recorded for **6** and **7**, respectively. These exocyclic C–*H* resonances were downfield shifted compared with the open-chain (6.24 ppm) or cyclic (5.92–6.25 ppm) olefinic C*H*s for our recently reported tantalum complexes (Scheme 2a).[12] Such a deshielded exocyclic proton is indicative of an aromatic environment.[5] The ^{13}C{^{1}H} NMR spectrum of **5** displayed the signals of $C_\alpha(3)$, $C_\beta(4)$, $C_\gamma(5)$, and $C_\delta(6)$ at 222.4, 92.7, 127.9, and 141.7 ppm, respectively. The down-field C_α chemical shift suggested a carbenoid character. The ^{11}B{^{1}H} NMR spectrum of **5** displayed a 2 : 3 : 2 : 3 pattern ranging from −2.4 to −11.1 ppm. The solution NMR data of **6** and **7** are consistent with those of **5** (Table 1).

The UV-vis spectra of **5**, **6**, and **7** (Fig. S19–S21 in the ESI†) showed the maximum absorption wavelengths λ_{max} at 481, 480, and 491 nm, which fall in the visible light region and account for the dark colours of these complexes.

According to the structural and spectroscopic data, the overall bonding pictures of the metallabicyclic moiety in **5–7** can be described as a resonance hybrid of forms **A**, **B**, **C**, and **D**. (Scheme 2b). Structure **A** stands for the chelated vinyl amide form of the metallacyclic system without M–N d_π–p_π interaction, while structures **B** and **C** demonstrate the M–N d_π–p_π interaction that leads to trigonal planar geometry for both nitrogen atoms. Structures **C** and **D** account for the delocalisation over the tantallapyridinium ring, in which structure **D** demonstrates the carbene character of $C_\alpha(3)$, consistent with the downfield resonance observed from ^{13}C NMR spectra (Table 1).

Computational studies

Concerning the co-planar structures of **5–7** with considerable bond length equalisation, we wondered whether the tantallapyridinium and tantallaazirine units are aromatic. To address this issue, we employed density functional theory (DFT) using the ωB97XD functional (see the ESI† for computational details) to calculate the nucleus-independent chemical shift (NICS) values for **5**, which are normally used as a measure of aromaticity.[19] NICS(0)/NICS(1)/NICS(1)$_{zz}$ values of −12.3/−13.9/−22.2 and −4.3/−7.8/−31.9 ppm were obtained for the tantallapyridinium (**b**) and tantallaazirine (**a**) rings, respectively (Scheme 3a). While the negative NICS values of the 3-membered tantallaazirine ring are attributable to the influence of anisotropy around the metal,[4c] the large negative NICS(1)$_{zz}$ value of the 6-membered tantallapyridinium ring points to the metallaaromatic character.[19]

The aromaticity of the tantallapyridinium ring in **5** is further supported by anisotropy of the induced current density (ACID) analyses. ACID is a powerful computational descriptor to visualise the delocalisation of electrons within a molecule as well as induced currents in an external magnetic field[20] and has been widely used for evaluation of metallaaromaticity.[4c,5g] As shown in Scheme 3b, the connectivity of the ACID isosurface suggests considerable electron delocalisation over the metallabicyclic moiety in **5**. When a magnetic field pointing perpendicular upwards to the tantallapyridinium plane is placed, the induced current vectors, plotted as red-head green arrows on the ACID surface, display a clockwise, diatropic ring circulation (Scheme 3b). Such a diatropic-induced current is evidence of aromaticity and is consistent with the NMR deshielding for exocyclic protons and the NICS calculation.

Aromatic stabilisation energy (ASE), calculated as the reaction energy of isodesmic reactions, is another useful criterion for aromaticity, since an aromatic molecule is usually more stable than its other isomers.[21] We proposed a hypothetical isodesmic reaction for **5** using the "methyl–methylene" isomerisation method recommended by Schleyer,[21] to estimate the ASE of **5** (Scheme 3c). An aromatic stabilisation energy (ASE) of 14.5 kcal mol^{-1} was obtained by considering the relative stability of **5** with respect to the isomeric structure (**5′**) (Scheme 3c). The calculated ASE value is comparable to those reported for rhenabenzenes.[22]

To further understand the mechanistic details for the formation of **5–7**, we calculated the energy profile for the reaction of **2** with two equiv. of XylNC leading to the formation of **5** (Scheme 4). Coordination of the first molecule of XylNC to **2** is the initial event of the reaction and is slightly exergonic with a small barrier, as expected. The coordination is followed by the insertion of the coordinated XylNC to the Ta–Me bond to give η^2-iminoacyl η^2-alkyne complex **E**.[12] These two steps are very facile and exergonic by 28.9 kcal mol^{-1}. The C–C bond formation contributes significantly to the stability of **E**. Since **E** is formally a 16 e$^-$ species, further coordination of the second equiv. of XylNC to **E** is possible, but at a stability penalty to give **E′**. Clearly, the further coordination promotes reductive coupling of the two η^2 ligands, leading to the formation of the 5-membered metallacyclic complex **F**. Again, the C–C bond formation contributes significantly to the high stability of **F**. From **F**, a very facile insertion of the second coordinated XylNC into Ta–C gives **G** with an *exo* =NXyl unit. Coordination of the *exo* =NXyl unit to the metal centre followed by a very facile

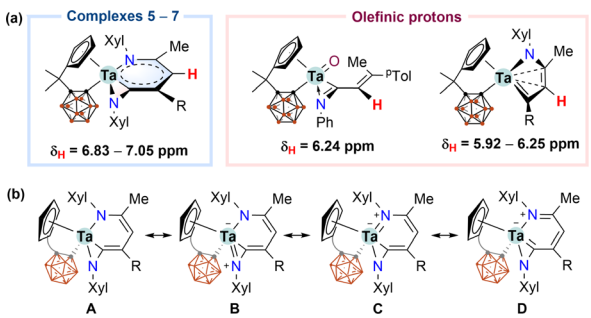

Scheme 2 (a) ^{1}H NMR chemical shifts for exocyclic C^5H protons in **5–7** and for olefinic protons; (b) resonance structures of **5–7**.

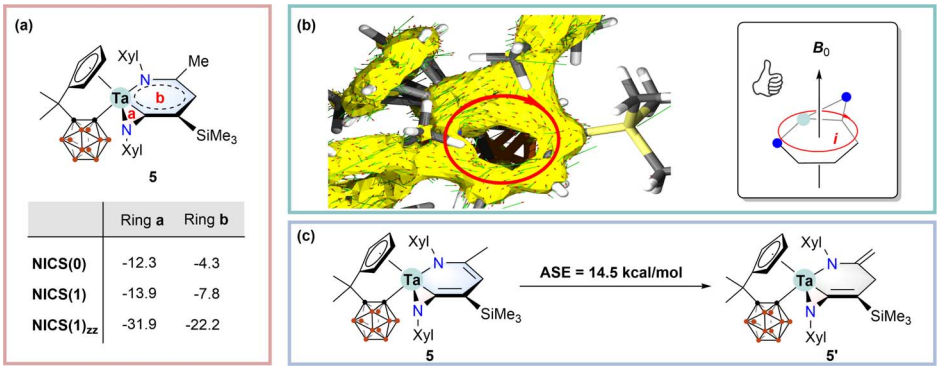

	Ring a	Ring b
NICS(0)	-12.3	-4.3
NICS(1)	-13.9	-7.8
$NICS(1)_{zz}$	-31.9	-22.2

Scheme 3 (a) Calculated nucleus-independent chemical shifts (NICSs, in ppm) for the tantallaazirine and tantallapyridinium rings in **5**; (b) calculated ACID for 5 with a magnetic field pointing upward the ring plane. The yellow surface is the ACID isosurface plotted in 0.05 isovalue, and the small red-head green arrows are current density vectors. The subgraph on the right side illustrates the left-hand relationship between the external magnetic field and the induced ring current; (c) calculation of the aromatic stabilisation energy (ASE) for **5**.

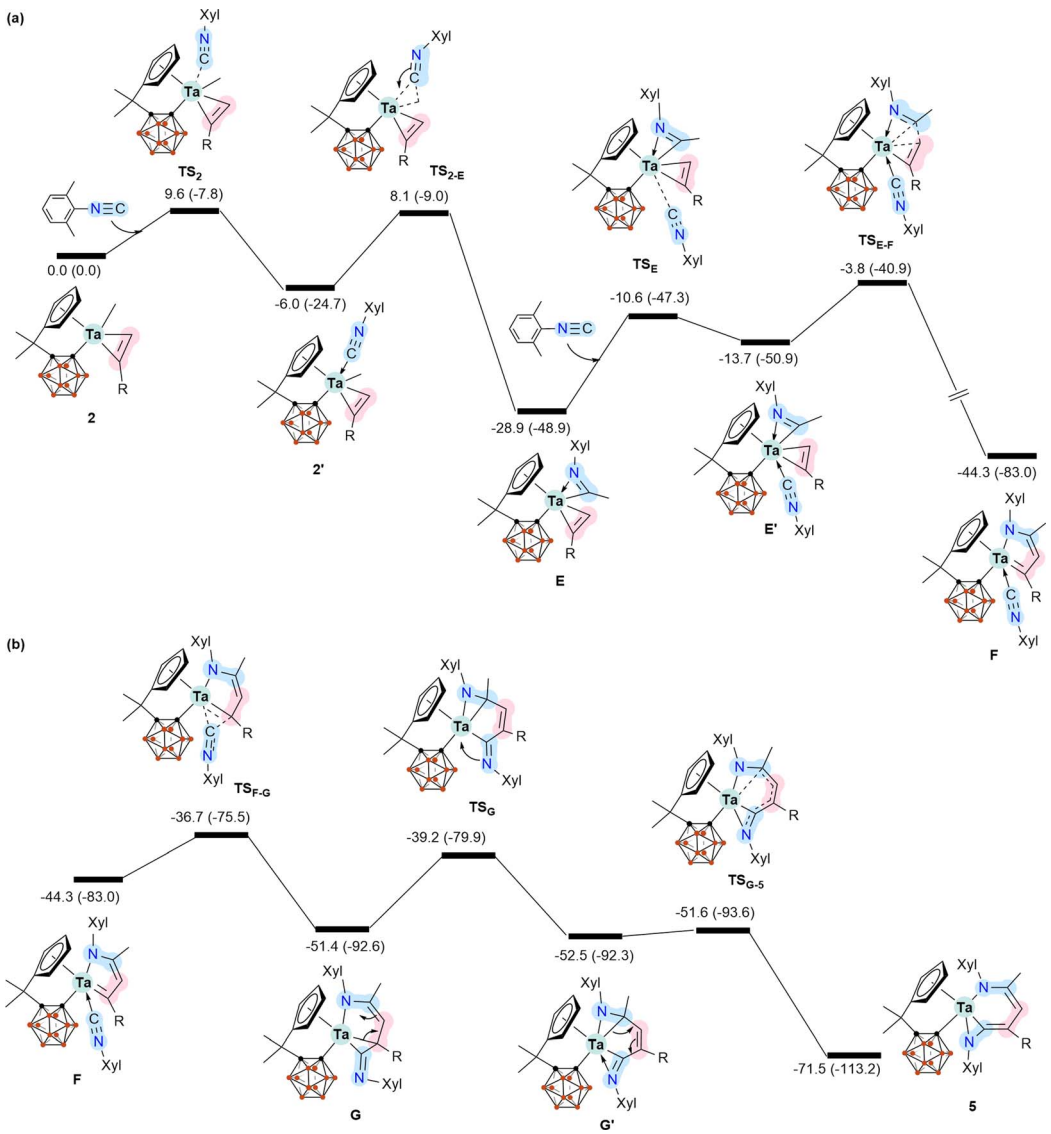

Scheme 4 Energy profile calculated for the reaction of **2** with two molecules of XylNC leading to the formation of **5**. For clarity, the energy profile is separated into two parts (a and b). The relative free energies and electronic energies (in parentheses) are given in kcal mol^{-1}.

structural rearrangement gives the final product **5**. The calculation results indicate that the formation of **5** is very exergonic by 71.5 kcal mol^{-1}, and the reductive coupling of the two η^2 ligands is rate-determining with an overall barrier of 25.1 kcal mol^{-1}.

Conclusions

We have successfully synthesised three tantallapyridinazirine complexes (**5–7**) bearing a linked cyclopentadienyl–carboranyl ligand *via* treating tantalum alkyne complexes with two equiv. of isocyanide. The aromaticity of the resultant tantallapyridinium ring is evidenced by the planar structure, equalised bond lengths, and the deshielded exocyclic proton signal in ^{1}H NMR. Such aromaticity has also been supported by DFT calculations. Complexes **5–7** represent the first examples of metallaaromatics involving d^0 early transition metal ions. This work also offers a new venue for the synthesis of such kinds of complexes.

Data availability

The datasets supporting this article have been uploaded as part of the ESI.†

Author contributions

Z. L. and Z. X. directed and conceived this project. J. Y. conducted the experiments. X. X. performed the theoretical work. All authors discussed the results and wrote the manuscript.

Conflicts of interest

There are no conflicts to declare.

Acknowledgements

This work was supported by grants from the Research Grants Council of HKSAR (Project No. SRFS2021-4S05 to Z. X. and 16302222 to Z. L.) and the Southern University of Science and Technology (to Z. X.).

Notes and references

1 M. Faraday, *Philos. Trans. R. Soc. London*, 1825, **115**, 440.
2 (*a*) F. A. Kekulé, *Bull. Soc. Chim. Fr.*, 1865, **3**, 98; (*b*) F. A. Kekulé, *Bull. Acad. R. Med. Belg.*, 1865, **19**, 551.
3 D. L. Thorn and R. Hoffmann, *Nouv. J. Chim.*, 1979, **3**, 39.
4 (*a*) H. S. Rzepa, *Chem. Rev.*, 2005, **105**, 3697; (*b*) I. Fernández and G. Frenking, *Chem.–Eur. J.*, 2007, **13**, 5873; (*c*) G. Periyasamy, N. A. Burton, I. H. Hillier and J. M. H. Thomas, *J. Phys. Chem. A*, 2008, **112**, 5960; (*d*) I. Fernández, G. Frenking and G. Merino, *Chem. Soc. Rev.*, 2015, **44**, 6452; (*e*) D. Chen, Q. Xie and J. Zhu, *Acc. Chem. Res.*, 2019, **52**, 1449; (*f*) D. W. Szczepanik and M. Solà, *ChemistryOpen*, 2019, **8**, 219; (*g*) B. J. R. Cuyacot, Z. Badri, A. Ghosh and C. Foroutan-Nejad, *Phys. Chem. Chem. Phys.*, 2022, **24**, 27957.
5 Selected reviews for metallaaromatic compounds: (*a*) J. R. Bleeke, *Acc. Chem. Res.*, 2007, **40**, 1035; (*b*) B. J. Frogley and L. J. Wright, *Chem.–Eur. J.*, 2018, **24**, 2025; (*c*) G. Jia, *Acc. Chem. Res.*, 2004, **37**, 479; (*d*) J. Wei, W.-X. Zhang and Z. Xi, *Chem. Sci.*, 2018, **9**, 560; (*e*) C. Zhu and H. Xia, *Acc. Chem. Res.*, 2018, **51**, 1691; (*f*) D. Chen, Q. Xie and J. Zhu, *Acc. Chem. Res.*, 2019, **52**, 1449; (*g*) D. Chen, Y. Hua and H. Xia, *Chem. Rev.*, 2020, **120**, 12994; (*h*) Y. Zhang, C. Yu, Z. Huang, W.-X. Zhang, S. Ye, J. Wei and Z. Xi, *Acc. Chem. Res.*, 2021, **54**, 2323; (*i*) M. Luo, D. Chen, Q. Li and H. Xia, *Acc. Chem. Res.*, 2023, **56**, 924.
6 Selected articles for aromatic metallabenzenes: (*a*) G. P. Elliott, W. R. Roper and J. M. Waters, *J. Chem. Soc. Chem. Commun.*, 1982, 811; (*b*) J. R. Bleeke, Y. F. Xie, W. J. Peng and M. Chiang, *J. Am. Chem. Soc.*, 1989, **111**, 4118; (*c*) V. Jacob, T. J. R. Weakley and M. M. Haley, *Angew. Chem., Int. Ed.*, 2002, **41**, 3470; (*d*) H. Zhang, H. Xia, G. He, T. B. Wen, L. Gong and G. Jia, *Angew. Chem., Int. Ed.*, 2006, **45**, 2920; (*e*) K. C. Poon, L. Liu, T. Guo, J. Li, H. H. Y. Sung, I. D. Williams, Z. Lin and G. Jia, *Angew. Chem., Int. Ed.*, 2010, **49**, 2759.
7 Selected articles for aromatic metallapyridines or metallapyridiniums: (*a*) B. Liu, H. Wang, H. Xie, B. Zeng, J. Chen, J. Tao, T. B. Wen, Z. Cao and H. Xia, *Angew. Chem., Int. Ed.*, 2009, **48**, 5430; (*b*) Y. Wang, Y. Sun, W. Bai, Y. Zhou, X. Bao and Y. Li, *Dalton Trans.*, 2022, **51**, 2876.
8 Z. Huang, Y. Zhang, W.-X. Zhang, J. Wei, S. Ye and Z. Xi, *Nat. Commun.*, 2021, **12**, 1319.
9 (*a*) D. B. Lawson and R. L. DeKock, *J. Phys. Chem. A*, 1999, **103**, 1627; (*b*) B. T. Psciuk, R. L. Lord, C. H. Winter and H. B. Schlegel, *J. Chem. Theory Comput.*, 2012, **8**, 4950; (*c*) J. R. Kummer and J. M. Brom, *J. Phys. Chem. A*, 2016, **120**, 10007; (*d*) M. Mauksch and S. B. Tsogoeva, *Chem.–Eur. J.*, 2018, **24**, 10059.
10 (*a*) K. J. Weller, I. Filippov, P. M. Briggs and D. E. Wigley, *Organometallics*, 1998, **17**, 322; (*b*) S. D. Gray, K. J. Weller, M. A. Bruck, P. M. Briggs and D. E. Wigley, *J. Am. Chem. Soc.*, 1995, **117**, 10678; (*c*) T. H. Perera, R. L. Lord, M. J. Heeg, H. B. Schlegel and C. H. Winter, *Organometallics*, 2012, **31**, 5971.
11 R. D. Profilet, P. E. Fanwick and I. P. Rothwell, *Angew. Chem., Int. Ed.*, 1992, **31**, 1261.
12 J. Yang and Z. Xie, *Organometallics*, 2023, **42**, 1347.
13 (*a*) Z. Xie, *Acc. Chem. Res.*, 2003, **36**, 1; (*b*) Z. Xie, *Coord. Chem. Rev.*, 2006, **250**, 259; (*c*) H. Shen and Z. Xie, *Chem. Commun.*, 2009, 2431.
14 H. Tsurugi, Z. Qiu, K. Yamamoto, R. Arteaga-Muller, K. Mashima and Z. Xie, *Organometallics*, 2011, **30**, 5960.
15 (*a*) M. R. Churchill, F. J. Hollander and R. R. Schrock, *J. Am. Chem. Soc.*, 1978, **100**, 647; (*b*) K. Mashima, H. Yonekura, T. Yamagata and K. Tani, *Organometallics*, 2003, **22**, 3766; (*c*) I. de Castro, J. de la Mata, M. Gómez, P. Gómez-Sal, P. Royo and J. M. Selas, *Polyhedron*, 1992, **11**, 1023.
16 J. R. Strickler, P. A. Wexler and D. E. Wigley, *Organometallics*, 1988, **7**, 2067.

17 A. S. Batsanov, A. V. Churakov, J. A. K. Howard, A. K. Hughes, A. L. Johnson, A. J. Kingsley, I. S. Neretin and K. Wade, *J. Chem. Soc., Dalton Trans.*, 1999, 3867.
18 (*a*) N. C. Tomson, J. Arnold and R. G. Bergman, *Dalton Trans.*, 2011, **40**, 7718; (*b*) N. C. Tomson, J. Arnold and R. G. Bergman, *Organometallics*, 2010, **29**, 2926.
19 Z. Chen, C. S. Wannere, C. Corminboeuf, R. Puchta and P. v. R. Schleyer, *Chem. Rev.*, 2005, **105**, 3842.
20 D. Geuenich, K. Hess, F. Köhler and R. Herges, *Chem. Rev.*, 2005, **105**, 3758.
21 P. v. R. Schleyer and F. Pühlhofer, *Org. Lett.*, 2002, **4**, 2873.
22 R. Lin, K.-H. Lee, K. C. Poon, H. H. Y. Sung, I. D. Williams, Z. Lin and G. Jia, *Chem.–Eur. J.*, 2014, **20**, 14885.